



HAL
open science

Candida albicans strains adapted to the mouse gut are resistant to bile salts via a Flo8-dependent mechanism

Susana Hidalgo-Vico, Daniel Prieto, Rebeca Alonso-Monge, Elvira Román, Corinne Maufrais, Christophe D'Enfert, Jesús Pla

► To cite this version:

Susana Hidalgo-Vico, Daniel Prieto, Rebeca Alonso-Monge, Elvira Román, Corinne Maufrais, et al.. Candida albicans strains adapted to the mouse gut are resistant to bile salts via a Flo8-dependent mechanism. Fungal Genetics and Biology, 2024, 175, pp.103939. 10.1016/j.fgb.2024.103939 . pasteur-04843479

HAL Id: pasteur-04843479

<https://pasteur.hal.science/pasteur-04843479v1>

Submitted on 17 Dec 2024

HAL is a multi-disciplinary open access archive for the deposit and dissemination of scientific research documents, whether they are published or not. The documents may come from teaching and research institutions in France or abroad, or from public or private research centers.

L'archive ouverte pluridisciplinaire **HAL**, est destinée au dépôt et à la diffusion de documents scientifiques de niveau recherche, publiés ou non, émanant des établissements d'enseignement et de recherche français ou étrangers, des laboratoires publics ou privés.



Distributed under a Creative Commons Attribution - NonCommercial - NoDerivatives 4.0 International License



Regular Articles

Candida albicans strains adapted to the mouse gut are resistant to bile salts via a Flo8-dependent mechanism

Susana Hidalgo-Vico^{a,1}, Daniel Prieto^{a,1}, Rebeca Alonso-Monge^a, Elvira Román^a, Corinne Maufrais^{b,c}, Christophe d'Enfert^b, Jesús Pla^{a,*}

^a Departamento de Microbiología y Parasitología-IRYCIS, Facultad de Farmacia, Universidad Complutense de Madrid, Avda. Ramón y Cajal s/n, 28040 Madrid, Spain

^b Institut Pasteur, Université Paris Cité, INRAE USC2019, Unité Biologie et Pathogénicité Fongiques, Département de Mycologie, 75015 Paris, France

^c Institut Pasteur, Université Paris Cité, Hub de Bioinformatique et Biostatistique, Centre de Ressources et Recherche en Informatique (C2RI), 75015 Paris, France



ARTICLE INFO

Keywords:

Candida albicans
Colonization
Evolution
Adaptation
Filamentation

ABSTRACT

Candida albicans normally colonizes the human gastrointestinal tract as a commensal. Studying fungal factors involved in colonizing the mammalian gastrointestinal tract requires mouse models with altered microbiota. We have obtained strains of *C. albicans* through microevolution in the mouse gut for a prolonged period (one year) that display a substantial increase in fitness in this niche. These strains show resistance to bile salts, an increase in their adhesion to the intestinal mucosa, and are unable to filament in response to serum. Genetic analysis revealed some alterations, mainly a triploidy of chr7, a whole chr6 homozygosity, and an SNP in the *FLO8* gene (located in the chr6), resulting in a truncated protein version. A wild type *FLO8* gene complemented filamentation and bile salt sensitivity but showed an intermediate fitness phenotype in colonization. Alterations in bile salt sensitivity were also evident in *bmt* mutants, defective in β -mannosylation, and transcriptional targets of Flo8, suggesting a link between the fungal cell wall and mammalian gut colonization via the Flo8 transcriptional regulator.

1. Introduction

The dimorphic fungus *Candida albicans* colonizes the vaginal and gastrointestinal tracts of humans, where it behaves as a harmless commensal; however, it can translocate to other regions of the human body causing severe diseases when the host is immunocompromised. Understanding the mechanisms that the fungus uses to colonize the mammalian gut is essential for developing strategies to control an undesired proliferation in this niche, thus blocking systemic dissemination.

Identifying *C. albicans* genes involved in colonizing the mammalian gastrointestinal tract normally requires mouse models with a reduction of the endogenous bacterial microbiota via antibiotic therapy (Koh, 2013). Fungal colonization and fitness are normally estimated by assessing either the viability of fungal cells (via CFU counting) or the DNA content (via qPCR) of the material recovered from the stools as well as by *post-mortem* analysis of the fungal load in the mouse intestine (Prieto and Pla, 2022). Fitness assays frequently involve competition experiments between two isogenic (mutant and wild-type) strains

(Neville et al., 2015; Prieto et al., 2016; Witchley et al., 2019). This methodology has allowed the identification of several regulators of colonization of very different natures, including genes regulating metabolic pathways, genes involved in signaling pathways, and certain morphogenetic regulators (Noble, 2013; Perez et al., 2013; Pierce and Kumamoto, 2012; Ramírez-Zavala et al., 2017; Román et al., 2018; Vautier et al., 2015).

Adaptation to the commensal status has been suggested to be mediated by Wor1 (Pande et al., 2013) the master regulator of the white opaque (wo) transition (Huang et al., 2006; Srikantha et al., 2006), an environmentally regulated epigenetic transition that prepares cells for mating (Soll, 2014). Wor1 was also proposed to mediate the conversion to the GUT morphotype (from Gastrointestinally induced Transition), a specialized type of cell adapted to the mammalian gut. Wor1 also regulates Efg1 (Stoldt et al., 1997), a transcriptional regulator involved in the wo transition (Sonneborn et al., 1999) as well as in the fitness in the gastrointestinal tract of mice (Pierce and Kumamoto, 2012).

By using a microevolution selection strategy, *C. albicans* strains with

* Corresponding author.

E-mail address: jpla@ucm.es (J. Pla).

¹ Both authors contributed equally to the work.

increased fitness have been isolated and shown to have reduced filamentation due to mutations in the *FLO8* gene (Tso et al., 2018). *FLO8* encodes a transcriptional regulator that acts downstream of the cAMP/PKA pathway and is involved in hyphal and biofilm formation and virulence (Cao et al., 2006; Fox et al., 2015; Liu et al., 2015). This gene is part of a transcriptional complex with Mfg1 and Mss11 and mediates chromosomal rearrangements that can restore filamentation in specific morphogenetic mutants (Polvi et al., 2019). Flo8 is also an important mediator of CO₂-induced morphogenesis and overexpression of the *FLO8* gene leads to hypersensitization to CO₂ levels (Du et al., 2012). Flo8 also participates in the **w** transition while SUMOylation of Wor1 occurs via the SUMO E3 ligase Wos1, a downstream effector of Flo8 (Yan et al., 2015), thus supporting a role in colonization. Mutations in *FLO8* that affect its binding to target genes have also been observed among clinical strains isolated from patients with vaginitis, a clinically relevant niche in *C. albicans* commensalism (Liu et al., 2015). Other transcription factors (like Rtg1, Rtg3, Tye7, Lys144, Zcf21, and Hms1) have been found to mediate commensalism by different regulatory circuits that control relevant metabolic traits (Perez et al., 2013). Downregulation of Efg1 or other regulators that induce filamentation like Ume6 conferred higher fitness in gastrointestinal colonization (Liang et al., 2019; Pierce et al., 2013; Pierce and Kumamoto, 2012) supporting the idea that filamentation would somehow impair commensal establishment in the gut. Certain hyphal proteins such as Als1, Als3, and Hwp1 are produced by *C. albicans* colonizing cells and promote an adaptive immune response that generates a specific sIgA response against those adhesins (Doron et al., 2021; Ost et al., 2021). These adhesins that are predominantly expressed during hyphal growth may promote adhesion to the intestine (de Groot et al., 2013; Hoyer and Cota, 2016) although little in vivo data using in vivo or ex vivo models have been obtained.

Given the complexity of the environment of the mammalian gut, not

only fungus-derived elements are crucial for colonization but also host-derived factors. Gut microbiota plays a prominent role (Eckstein et al., 2020; Leonardi et al., 2018; Neville et al., 2015) but other chemical or physical conditions also influence *C. albicans* proliferation. One such chemical is bile, a complex fluid containing cholesterol, bile salts, and other compounds involved in lipid assimilation by the host. In principle, gut-residing microbes need to be well adapted to this substance which is therefore present in several laboratory media to facilitate their isolation. Candidiasis can result in bile duct obstruction (Domagk et al., 2001), and *C. albicans* present in the gall bladder may be refractory to some antifungal treatments (Hsieh et al., 2017), indicating the clinical relevance of sensitivity to bile salts in this fungus. Bile salts inhibit morphogenesis as well as adhesion of *C. albicans* cells to a colonic cancer line (Guinan et al., 2018) and certain mutants in genes involved in commensalism (mutants in the HOG pathway) are sensitive to bile salts (Prieto et al., 2014) as occurs with cells where *WOR1* is overexpressed (Prieto et al., 2017). Overexpression of the transcription factor *CRZ2* also results in increased fitness, bile salt resistance, and changes in phosphomannan composition (Znaidi et al., 2018).

We describe here the isolation of strains adapted to the mouse gut via experimental microevolution in this niche. These strains have chromosomal reorganizations leading to altered traits related to mammalian gut colonization that are caused, in part, by mutations in the *FLO8* gene. We also show that *flo8Δ* mutants have an increased resistance to bile salts that would be mediated, at least in part, by an altered cell wall mannosylation.

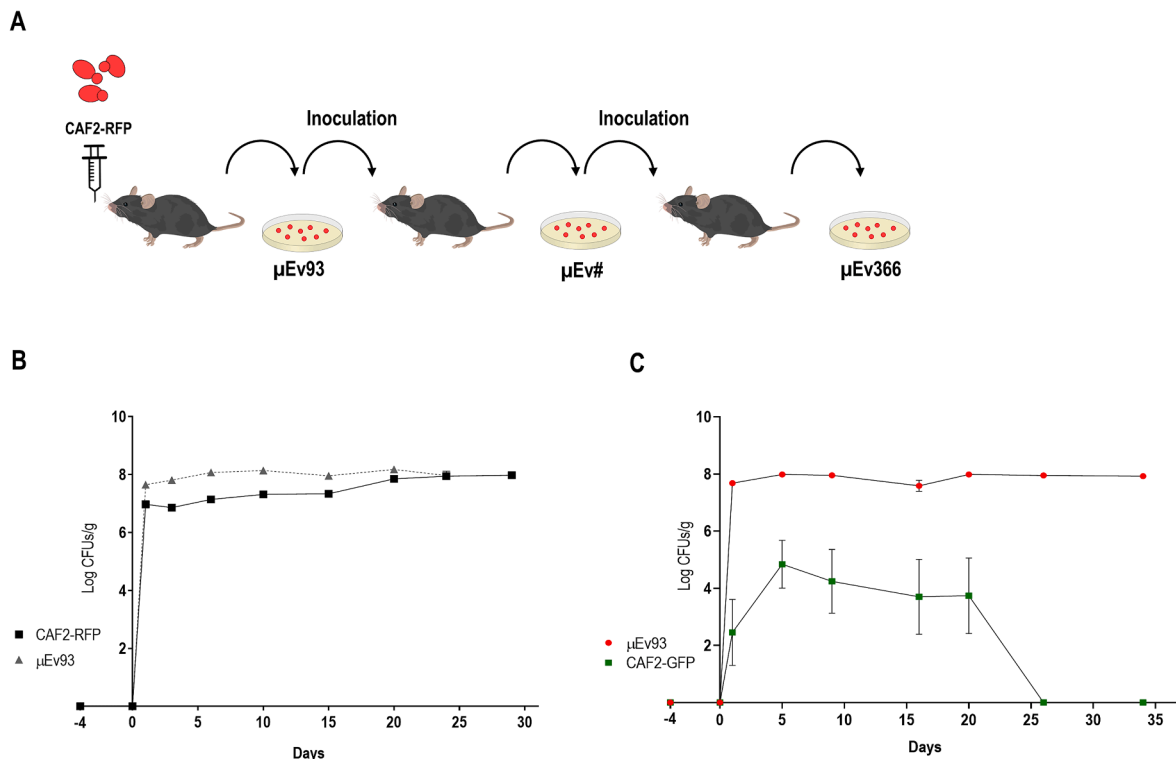


Fig. 1. Colonization of mouse gut by micro-evolved *C. albicans*. (A) Scheme of sequential *C. albicans* colonization procedure to obtain micro-evolved strains (μ Ev). (B) Colonization levels of CAF2-RFP (squares) and micro-evolved strain from day 93 (μ Ev93, triangles) colonizing separated groups. Data from CFU determination from stool samples (expressed as mean \pm SEM). Each data set corresponds to an independent group ($n = 2$). (C) Competition between CAF2-GFP (green) and μ Ev93 (red) strains colonization in C57BL/6 antibiotic-treated mice inoculated with a 1:1 mix of the indicated strains. Data from CFU determination from stool samples obtained from 7 mice in two independent experiments (expressed as mean \pm SEM). (For interpretation of the references to colour in this figure legend, the reader is referred to the web version of this article.)

2. Results

2.1. *C. albicans* strains micro-evolved in the mouse intestine display improved capacity of colonization

We generated strains with increased fitness to the mouse gut via experimental evolution in animals (Fig. 1A). For this purpose, an RFP-labelled *C. albicans* strain (CAF2-RFP) was sequentially inoculated by gavage in different groups of antibiotic-treated mice ($n = 2$) for up to one year (Material and Methods and Fig. 1A). After colonizing the mouse gastrointestinal tract for 7 to 9 weeks the *C. albicans* colonies obtained from stools were inoculated in a new group of mice. Strains were named according to the time of isolation from stools and called $\mu\text{Ev}\#$ (for # accumulated days). Cells appeared normal in morphology under standard laboratory growth conditions (Fig. S1). When inoculated the $\mu\text{Ev}93$ strain alone it showed an increase in fungal loads in stools in the first 10–15 days after gavage (Fig. 1B, triangles and dashed line) compared with those levels attained by the original CAF2-RFP strain inoculated alone (Fig. 1B, squares). We confirmed that these μEv strains showed increased ability to colonize the mouse gut since all $\mu\text{Ev}93$, $\mu\text{Ev}180$, and $\mu\text{Ev}366$ showed a significant increase in fitness compared to a GFP-labeled parental (CAF2-GFP) strain in co-colonization competition experiments (Figs. 1C, S2A and B). In these experiments, a CAF2-GFP control strain hardly attained colonization levels higher than 10^4 CFUs/g in stools, and levels were undetectable 3–4 weeks after gavage; in contrast, fungal loads for all micro-evolved strains were stable in the range of 10^8 CFUs/g as early as day 1 after oral administration (Figs. 1C, S2A and B). This increased fitness was maintained even after eleven *in vitro* passages of the micro-evolved strains in YPD medium at 37 °C (data not shown), indicating that it was not the result of a temporal transcriptional adaptation of the fungal cells to the intestine conditions.

2.2. The phenotype of hypercolonization in evolved strains is independent of *Wor1*

Overexpression of the *WOR1* gene has been shown to promote the conversion of white cells to opaque cells (Huang et al., 2006; Srikantha et al., 2006; Zordan et al., 2006). Given the relationship between *Wor1* and commensalism (Pande et al., 2013) we analyzed the staining of μEv strains with phloxine B (a compound that differentially stains opaque cells). As shown in Fig. 2A, all evolved strains showed increased staining with this compound. To study whether the underlying mechanisms favoring colonization in micro-evolved strains were *Wor1* dependent, we quantified the expression of *WOR1* in $\mu\text{Ev}93$, $\mu\text{Ev}180$, and $\mu\text{Ev}366$ cells growing *in vitro* in exponential phase by qPCR. All strains showed significant changes in *WOR1* expression (Fig. 2B) with a 6-fold increase compared to the original CAF2-RFP strain. To unambiguously determine the involvement of *WOR1* in adaptation to commensalism in those strains, *WOR1* was deleted in $\mu\text{Ev}93$ using CRISPR (see Material and Methods). Fungal colonization loads of a $\mu\text{Ev}93\text{-wor1}\Delta$ mutant were found like those obtained for the wild type or $\mu\text{Ev}93$ strains (around 10^{7-8} CFUs/g), and were consistently maintained over time (Fig. 2C). When fitness was assayed in competition experiments using CAF2-GFP as control, the levels of both strains mimicked those observed with the non-deleted strain (Figs. 2D and 1C). These results indicate that even though there are changes in *WOR1* expression in evolved strains, *WOR1* is not the main driver for the observed increased fitness.

2.3. Micro-evolved strains have reduced lipase and protease activity, and are resistant to bile salts

Different phenotypes were studied in the micro-evolved strains, especially those related to stresses that could in principle play a role in commensalism. Neither oxygen availability (growth in normoxia, microaerophilia, or anaerobiosis), osmotic stress (growth on NaCl-supplemented plates), nor oxidative stress (growth on hydrogen

peroxide-supplemented media) affected micro-evolved strains significantly compared to the parental CAF2-RFP strain. The use of alternative carbon sources (acetate, ethanol, glycerol, or citrate) also revealed no significant differences between evolved strains and the parental control (Fig. S3). However, $\mu\text{Ev}93$, $\mu\text{Ev}180$, and $\mu\text{Ev}366$ strains displayed reduced lipase and protease production *in vitro* as observed in specific egg yolk containing SEA or MEA media and BSA solid media, respectively (Fig. 3A and B). Additionally, we analyzed the resistance to bile salts as it can influence the behavior of intestinal microbes. As shown in Fig. 3C, all micro-evolved strains were resistant to 0.3 % bile salts when assayed on solid YPD medium compared to CAF2-RFP. Curiously, those strains were also resistant to azole drugs, although they did not display any difference against caspofungin compared with the parental strain (Fig. S3 and not shown). We also analyzed the adhesion of micro-evolved strains. Adhesion was checked on both abiotic (polystyrene) and biotic (gut mucosa) surfaces for the $\mu\text{Ev}93$ strain. This strain displayed a moderate, but significant, increase in adhesion to the mouse large intestine mucosa ($\text{ARI}=1.22 \pm 0.11$), in parallel with an important decrease in its adhesion to polystyrene ($\text{ARI}=0.36 \pm 0.08$) (Fig. 3D), an adhesion pattern that has already been observed in *C. albicans* strains altered in morphogenesis and colonization (Prieto et al., 2014; Román et al., 2023).

2.4. Genome sequencing reveals chromosomal alterations

Results presented above suggested that the increased fitness in μEv strains was inheritable. To identify the underlying genetic basis, we sequenced the genomes of strains CAF2-RFP, $\mu\text{Ev}93$, $\mu\text{Ev}180$, and $\mu\text{Ev}366$. Post-sequence cleanup and SNP calling were carried out and allele ratios at heterozygous sites (ABHet) were determined, allowing the identification of major chromosomal rearrangements, in particular aneuploidy and loss-of-heterozygosity events. This analysis revealed that the $\mu\text{Ev}93$ strain displayed a triploidy of chromosome 7, with two copies of haplotype A and one copy of haplotype B (Fig. 4A). Such triploidy was not present in the subsequent evolved strains ($\mu\text{Ev}180$ and $\mu\text{Ev}366$) that recovered diploidy of chromosome 7 (one copy of each haplotype A and B), suggesting that it was not responsible for the gain of fitness seen across the sequenced micro-evolved strains. In addition, all micro-evolved strains displayed a whole chromosome 6 homozygosity (Fig. 4B). Notably, these three strains were distinguished from the wild-type strain by a homozygous nonsense mutation in the chromosome 6-borne *FLO8* gene. A change from G to A mutates the glutamine 201-encoding TGG codon in the Flo8 protein to a TAG (STOP) in the *FLO8* gene. The *flo8*^{Q201*} allele was not present in the parental strain suggesting that it had arisen upon passage in the gastrointestinal tract and subsequently been brought to homozygosity due to whole-chromosome 6 loss-of-heterozygosity. It has been shown that a *C. albicans flo8* Δ mutant has defects in hyphal formation (Cao et al., 2006) while overexpression of *FLO8* leads to constitutive filamentation (Polvi et al., 2019). All evolved strains were unable to form filaments when growing in 5 % or 100 % FBS (fetal bovine serum), consistent with a *FLO8* altered genotype (Fig. 4C) and downregulates Flo8-dependent genes (Fig. S4).

2.5. *FLO8* wt allele causes sensitivity to bile salts

To define the role of *FLO8* in μEv strains, we constructed a genetic cassette to ectopically integrate a wild type *FLO8* allele at the neutral *NEUT5L* locus (Gerami-Nejad et al., 2013) under its native regulation. The defect in filamentation in a *flo8* Δ mutant was restored upon reintroduction of this construction under both sub-inducing (5 % FBS) and fully inducing (100 % FBS) conditions (Fig. 5A). *FLO8* reintegration in μEv strains ($\mu\text{Ev}\#\text{-pFLO8}$) also restored filamentation in the presence of both 5 % and 100 % FBS, although partially (Fig. 5A). Strain $\mu\text{Ev}93$ forms non-filamentous colonies on solid medium supplemented with BSA (Fig. 5B), a phenotype that was alleviated by integrating a wild-type copy of *FLO8*.

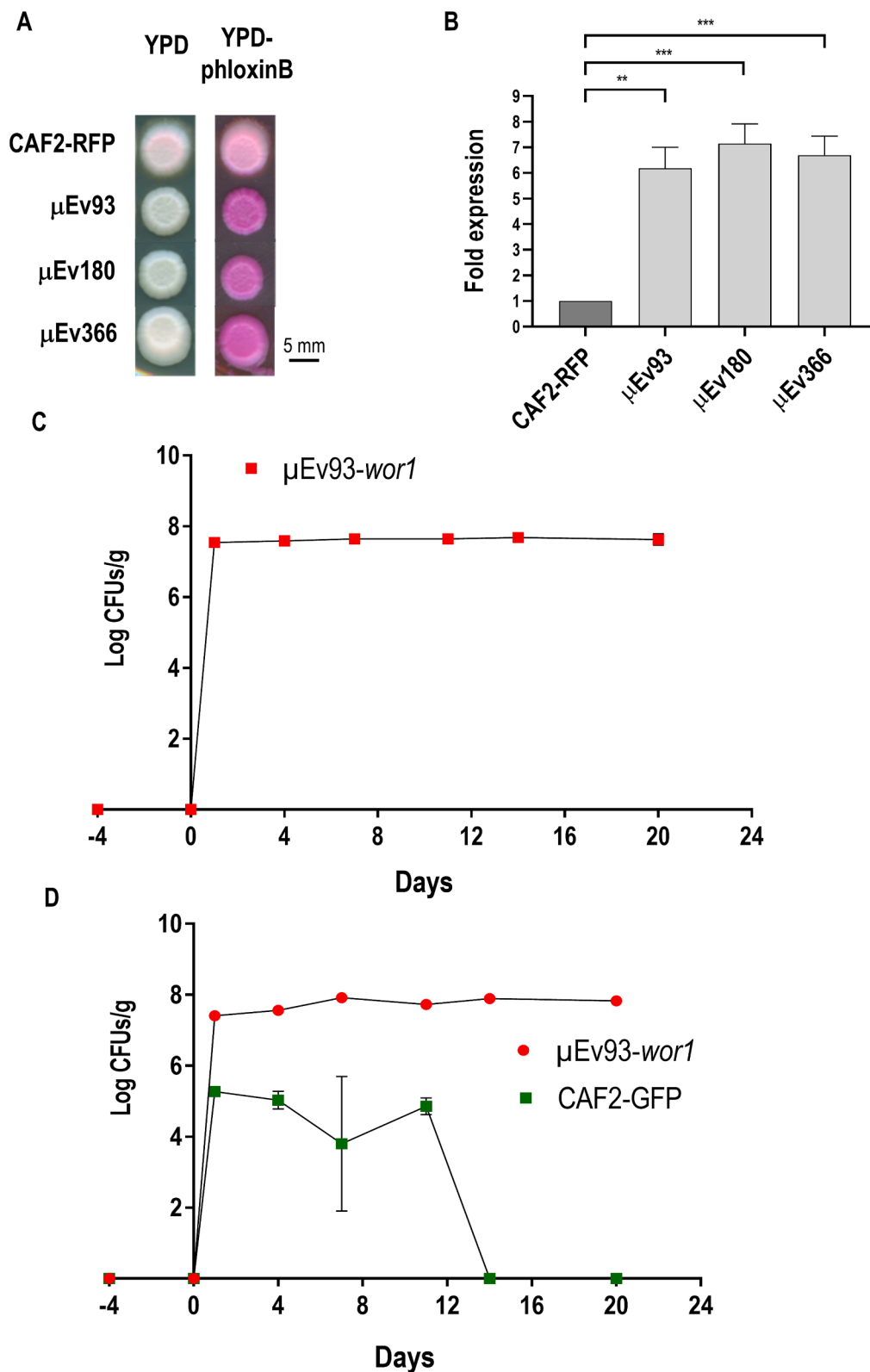


Fig. 2. Role of Wor1 in micro-evolved strains. (A) Phloxine B staining of CAF2-RFP and micro-evolved strains obtained after 93 days (μEv93), 180 (μEv180) days, or 366 days (μEv366) growing in YPD plates. (B) *WOR1* mRNA expression determined by qPCR in exponential phase cells from CAF2-RFP, μEv93, μEv180, and μEv366 strains. **p < 0.01, ***p < 0.001. (C) Colonization levels of μEv93 strain lacking *WOR1* gene (μEv93-wor1Δ, red). Data from CFU determination from stool samples obtained from 3 mice (expressed as mean ± SEM). (D) Competition in colonization between CAF2-GFP (green) and μEv93-wor1Δ strain (red). Mice were inoculated with a 1:1 mix of both strains. Data from CFU determination from stool samples obtained from 3 mice (expressed as mean ± SEM). (For interpretation of the references to colour in this figure legend, the reader is referred to the web version of this article.)

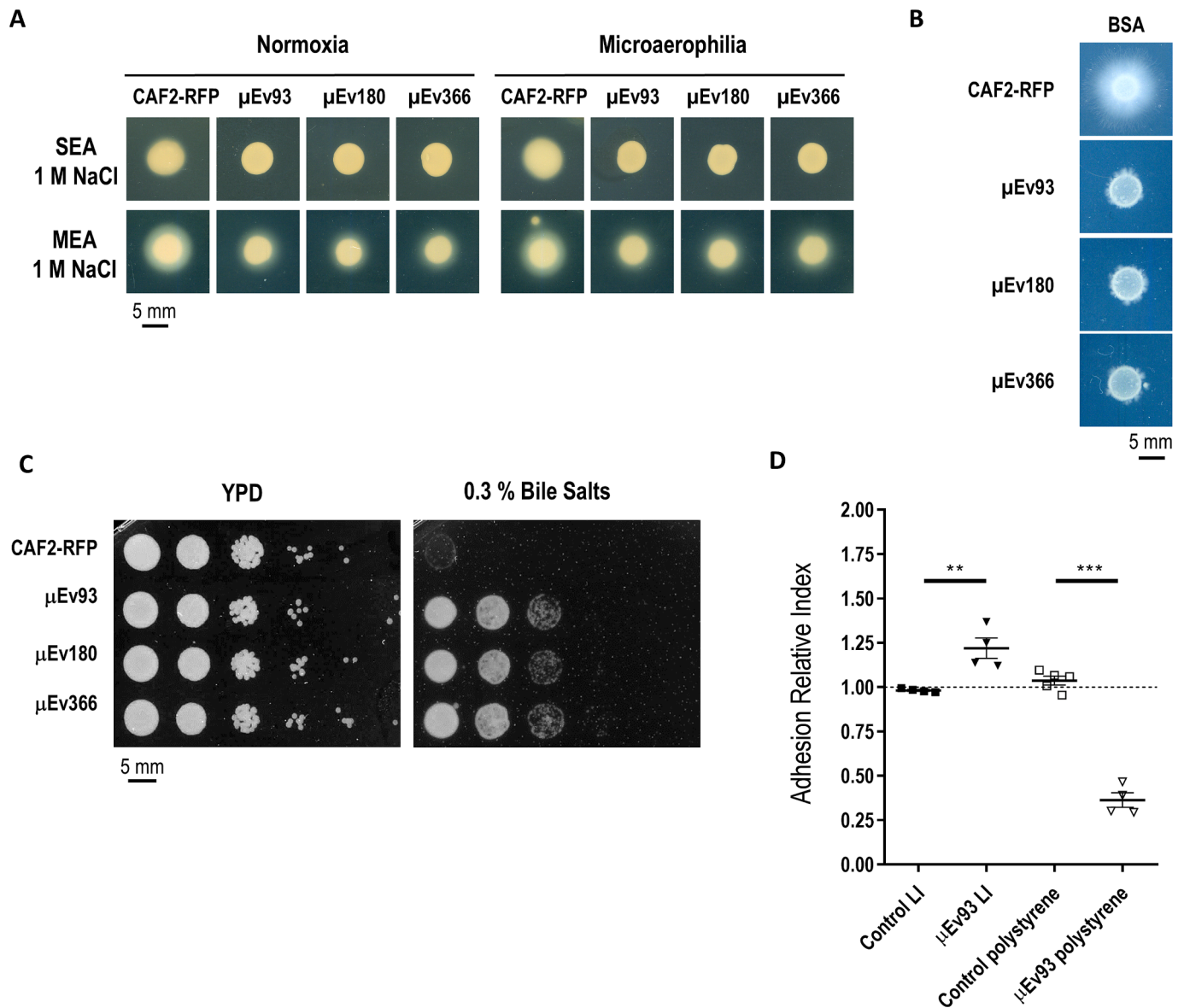


Fig. 3. Analysis of colonization-related phenotypes in micro-evolved strains. Determination of phospholipase (A) and protease (B) activity of CAF2-RFP, μEv93, μEv180, and μEv366 strains on SEA and MEA, or BSA agar plates under normoxia and microaerophilia atmosphere after 96 h at 37 °C. (C) Bile salts sensitivity of CAF2-RFP, μEv93, μEv180, and μEv366 strains. (D) Adhesion capacity of the μEv93 strain. The Adhesion Relative Index (ARI) is represented for μEv93 strain (using CAF2-GFP as internal control) in the large intestine (LI) and polystyrene. Individual values are shown with the mean ± SEM. An unpaired *t*-test was used for statistical analyses. ***p* < 0.01, ****p* < 0.001.

The reintroduction of *FLO8* abolished resistance to bile salts in all μEv strains (Figs. 6A and S5). A similar effect was also observed in a *flo8Δ* mutant (Fig. 6B) indicating that Flo8 influences this trait. Flo8 regulates the expression of a wide range of effector genes (Cao et al., 2006; Polvi et al., 2019). Among them, we found some members of the *BMT* family of genes that mediate β-mannosylation of cell wall proteins (Courjol et al., 2015; Polvi et al., 2019; Poulain and Jouault, 2004) that would affect bile sensitivity. According to Polvi et al. data, in a *flo8Δ* mutant *BMT2* gene is overexpressed (about 6-fold) at 37 °C, while *BMT4* and *BMT6* are repressed in those conditions (although *BMT4* down-regulation was not statistically significant). Therefore, the presence of Flo8 may reduce *Bmt2* levels. As shown in Fig. 6B, a *bmt2* mutant had increased sensitivity to bile salts compared to the control strain BWP17 (wt *FLO8* phenotype), while the *bmt4* and *bmt6* mutants were slightly more resistant than BWP17 (*flo8* mutant phenotype), thus suggesting a link between β-mannosylation of cell wall fungal proteins and resistance to bile salts. Bile salt resistance in the micro-evolved strains was not a

WOR1-dependent phenotype, as deletion of *WOR1* in these strains showed no changes compared to control cells while the reintroduction of a wild-type *FLO8* allele in *wor1Δ* mutant cells led to a bile salt-sensitive phenotype (Fig. S6).

Finally, to determine the role of *FLO8* in the colonization phenotypes observed for the micro-evolved strains, we performed competition colonization experiments between strain μEv93-pFLO8 and the CAF2-GFP parental strain. Even after the reintegration of the *FLO8* allele, μEv93-pFLO8 still showed an increase in fungal colonization compared with the CAF2 parental strain, with differences in fungal loads in the 10-fold range stable for more than a month (Fig. 6C). μEv93-pFLO8 was not able, however, to outcompete CAF2 in this assay. This colonization phenotype is significantly less drastic than the one observed before *FLO8* reintegration (see Fig. 1C), suggesting a main role for Flo8 alteration in the adaptation of μEv strains to the mouse gut.

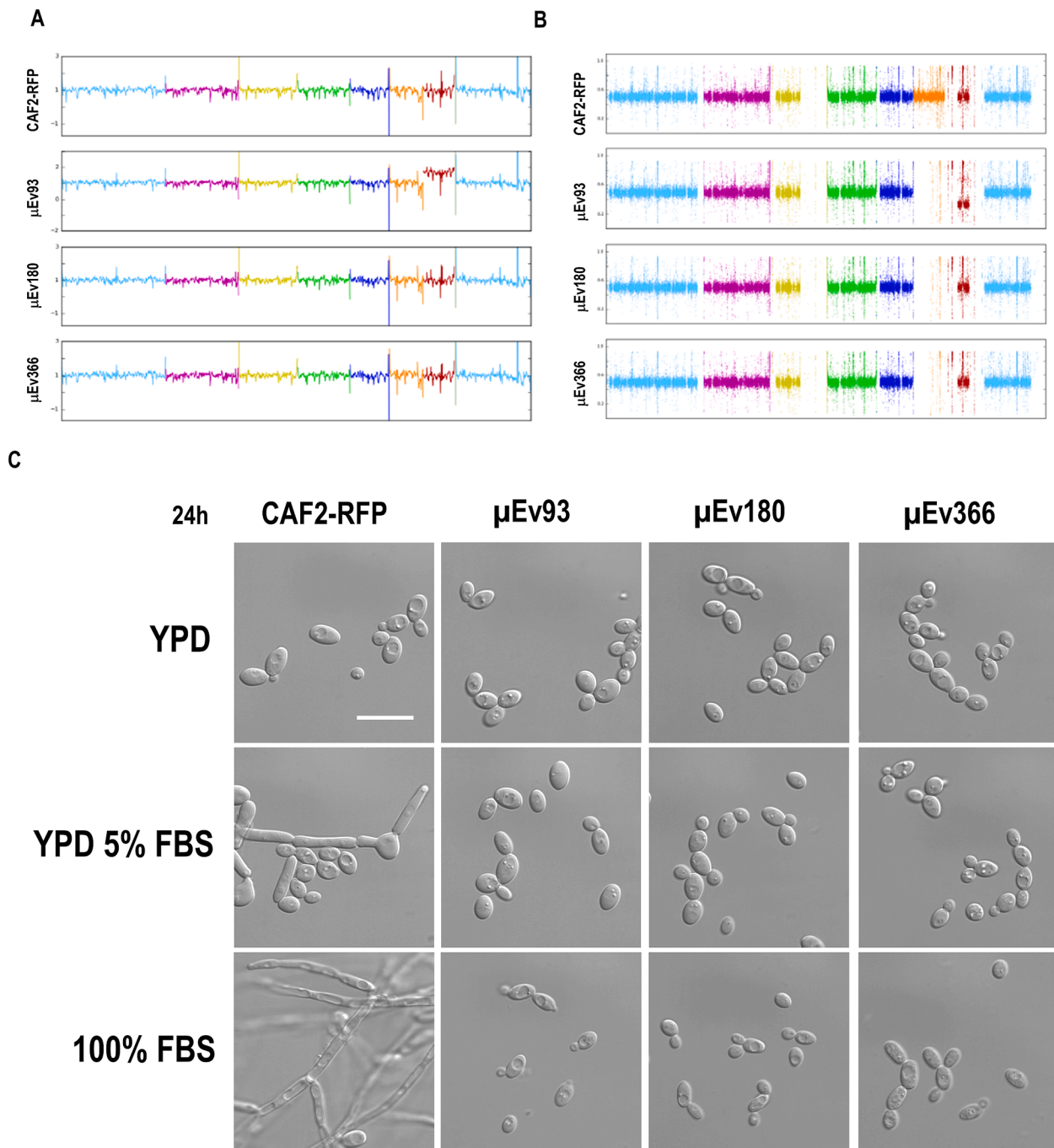


Fig. 4. Genetic alteration in micro-evolved strains. (A) Plots showing the normalized sequencing depth across the eight chromosomes in CAF2-RFP, μEv93, μEv180, and μEv366 strains. Sequencing reveals that all strains are diploid except strain μEv93 which displays a triploidy of chromosome 7 (brown). (B) Plots showing the allele balance at heterozygous positions across the eight chromosomes in CAF2-RFP, μEv93, μEv180, and μEv366 strains. Sequencing reveals homozygosity of chromosome 6 (orange) in all micro-evolved strains and confirms triploidy of chromosome 7 (brown) with two copies of haplotype A and one copy of haplotype B. (C) Filamentation ability of CAF2-RFP, μEv93, μEv180 and μEv366 strains growing in YPD, YPD supplemented with 5 % FBS or FBS alone after 24 h at 37 °C. The bar indicates 10 μm. (For interpretation of the references to colour in this figure legend, the reader is referred to the web version of this article.)

3. Discussion

Although *C. albicans* can cause relevant systemic infections in humans with impaired defenses, the common stage for this fungus is living in mucosa-related cavities, the intestine being the preferred niche. Analysis of the mechanisms for colonization of this niche is relevant as it is from there that most systemic candidiasis arises (Marco et al., 1999; Miranda et al., 2009; Zhai et al., 2020), when the host defenses (physical barriers, microbiota, immune system) are unable to control the

proliferation and translocation of the fungus to internal organs. Such analysis is also relevant as intestinal colonization by *C. albicans* has been reported to have positive effects in animal models (Alonso-Monge et al., 2021a), suggesting that colonization by this fungus is beneficial to the human host. Since rodents are not natural hosts for *C. albicans*, antibiotic therapy is required for colonization by this fungus (Bendel et al., 2002). We used this simplified model to generate strains that are more prone to colonization of the intestine in mice, obtaining *C. albicans* variants after a prolonged period (up to 1 year). We observed that 2–3 months of

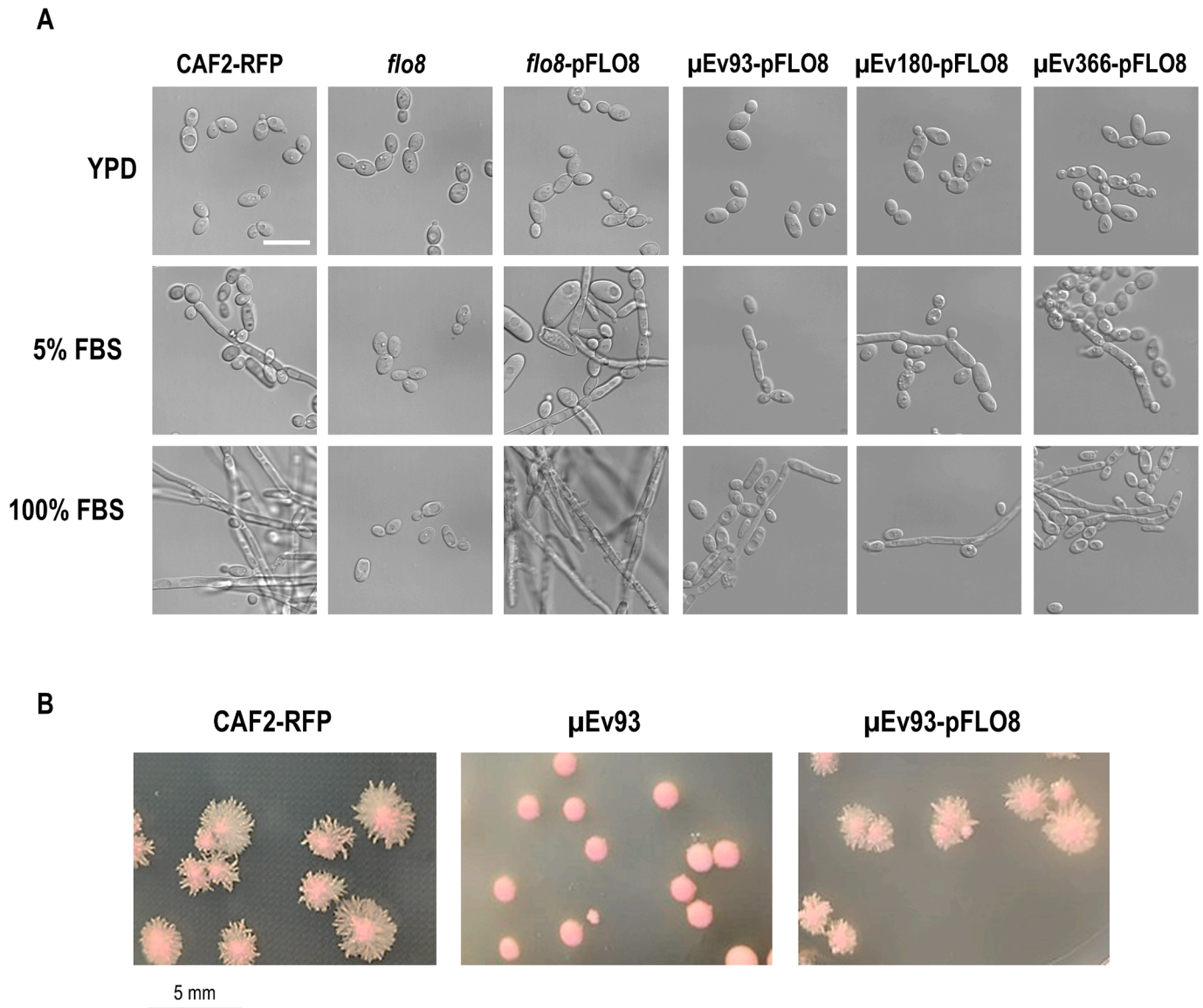


Fig. 5. Effect of *FLO8* reintegration in micro-evolved strains in filamentation. (A) Filamentation capacity of CAF2-RFP, *flo8* Δ mutant, and micro-evolved strains with the *FLO8* reintegrated allele (*flo8* Δ -pFLO8, μ Ev93-pFLO8, μ Ev180-pFLO8, μ Ev366-pFLO8) in YPD broth, YPD supplemented with 5 % FBS or FBS alone after 24 h at 37 °C. The bar indicates 10 μ m. (B) Colony morphology of the indicated strains on BSA agar plates after 96 h at 37 °C.

colonization are enough to generate both transient and stable genetic changes that enable increased fitness. Aneuploidies often arise in response to antifungals and other chemical stressors (Forche et al., 2009; Polvi et al., 2019; Selmecki et al., 2006; Selmecki et al., 2009) and have been reported as mechanisms of host adaptation and genetic diversity (Ene et al., 2018; Forche et al., 2018; Forche et al., 2019). In our evolution experiment, we identified a transient trisomy of chromosome 7 (only in μ Ev93), which has been previously observed either in nature (in clinical isolates) and in *Candida* cells passaged in the mouse model with apparently opposite outputs, which make it difficult to determine whether this trisomy confers a biological advantage for the fungus in the adaptation to this specific niche. Tso et al. (2018) showed no increased competitive fitness in 10 weeks (70d) micro-evolved strains (12 strains across 10 evolution lineages) harboring a Chr7 trisomy. Other groups, on the other hand, observed that strains evolved in the intestine for 42 days acquired an extra copy of Chr7 linked to an increased fitness, where 3 \times Chr7 strains outcompeted the 2 \times Chr7 parental strains (Kakade et al., 2023). These apparent discrepancies open the possibility that certain genetic changes may be not stable, but transitory during adaptation and

are more frequent in a certain range of time of micro-evolution (42d vs 70d vs >93d) that differ in the different laboratories. Some authors discuss that aneuploidies are usually unstable, and reversion to a euploid state is common once adaptation has been achieved (Bouchonville et al., 2009; Sun et al., 2023). Both loss-of-heterozygosity (LOH) and aneuploidy events have also been observed in the oral cavity where 24 h of infection in the OPC model was sufficient to induce genomic modifications. In this particular niche, both 3 \times Chr6 and 3 \times Chr5 were found to be the most frequent selected changes for the evolution to a commensal-like phenotype eliciting lower inflammatory host response while similar oral fungal burden than their 2 \times progenitors (Forche et al., 2018; Forche et al., 2019). Beyond large-scale genomic rearrangements, all three μ Ev93, μ Ev180, and μ Ev366 have a mutated *FLO8* allele in homozygosity due to the LOH of Chr6. This nonsense mutation *FLO8*^{Q201*} leads to a truncated protein that would keep minimal if any, functionality of the 792 amino-acid Flo8 protein. This specific mutation is different from those previously described after 8 or 10 weeks of colonization in the *FLO8* gene (also together with an LOH in Chr6) that leads to different frameshift or nonsense mutations (Tso et al., 2018). This region should

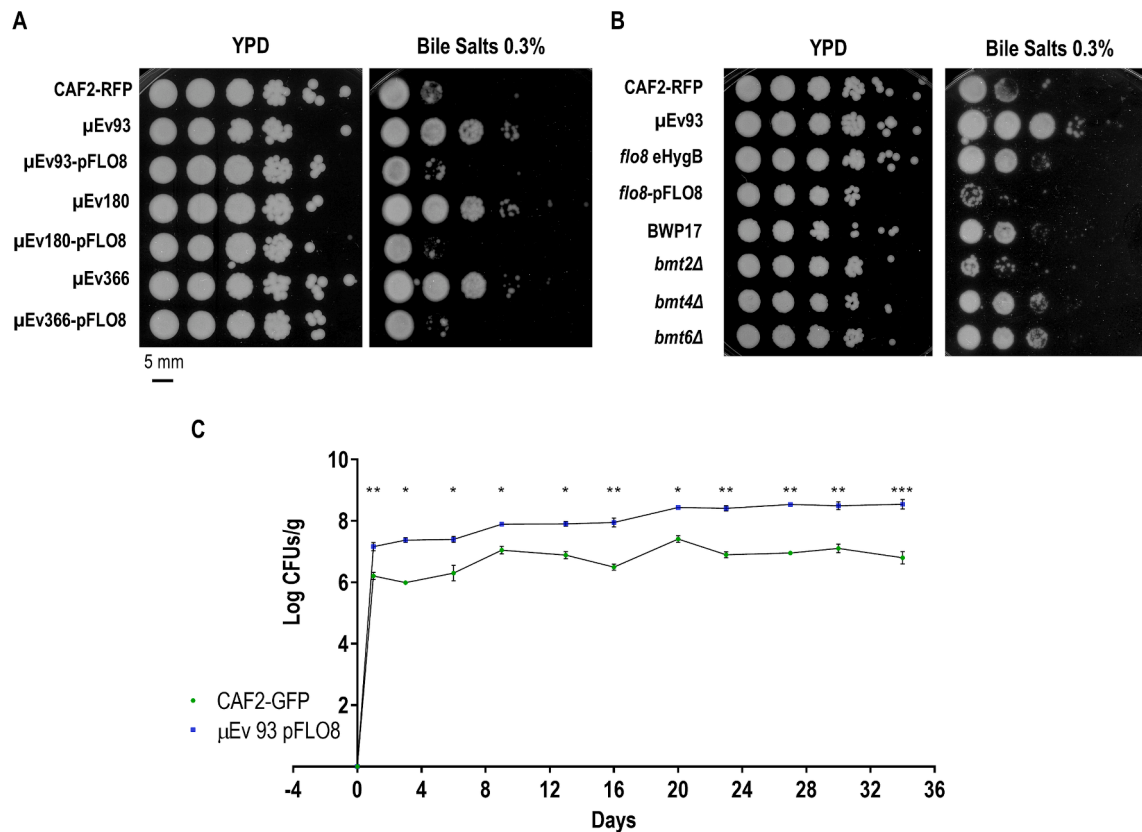


Fig. 6. Role of Flo8 in bile salt sensitivity and colonization of micro-evolved strains. Bile salts sensitivity of (A) micro-evolved strains with a reintegrated wt *FLO8* allele; (B) *flo8Δ* mutant with a reintegrated wt *FLO8* allele and mannosylation-related mutants. (C) Competition in colonization between CAF2-GFP (green) and μEv93-pFLO8 (blue) strains. Mice were inoculated with a 1:1 mix of both strains. Data from CFUs determination from stool samples obtained from 3 mice (expressed as mean ± SEM). Paired *t*-test was used for statistical analyses at each time point. **p* < 0.05, ***p* < 0.01, ****p* < 0.001. (For interpretation of the references to colour in this figure legend, the reader is referred to the web version of this article.)

be therefore considered a mutational hotspot since other *FLO8* allelic variations with five additional non-synonymous SNPs have been identified in *C. albicans* strains isolated from women with vulvovaginal candidiasis (Liu et al., 2015).

Micro-evolved strains were unable to produce hyphal growth even in the presence of 100 % FBS, behaving like a *flo8Δ* mutant (Cao et al., 2006). Even though other genetic alterations could contribute to the defects in filamentation, the integration of one copy of *FLO8* significantly restores the ability to filament in micro-evolved strains. Although evolution lineages may be different in humans, the yeast morphotype is important for adaptation to the murine niche (Román et al., 2018; Vautier et al., 2015) and *C. albicans* isolates that exhibit an increased fitness retain the ability to produce hyphae in the mice model of commensalism (Alonso-Monge et al., 2021b). *Wor1* is known to control the white/opaque switching and the conversion to GUT cells in *C. albicans* (Huang et al., 2006; Pande et al., 2013). *WOR1* overexpression has been recently described to block the yeast-to hypha transition in the presence of 100 % FBS and in *hog1* hyper filamentous mutants allowing the colonization of the murine intestine (Román et al., 2023). Therefore, it seemed reasonable to consider an influence of *Wor1* in the phenotype observed, especially since micro-evolved strains display a higher phloxine B staining (a characteristic of opaque and/or *WOR1* overexpressing cells). Micro-evolved strains displayed up to a 6-fold increase in *WOR1* mRNA levels however, interestingly, we did not observe GUT-like phenotype nor defects in alternative carbon source utilization (associated with *WOR1* overexpression (Hidalgo-Vico et al., 2022; Prieto et al., 2017). Although the enhanced level of *WOR1* expression observed in our micro-evolved strains may contribute to promoting gut colonization, deletion of the *WOR1* gene in the μEv93 strain maintained a high

colonization load and outcompeted its parental strain in the murine models indicating that adaptation to the gut is not due to this single factor.

To stably colonize *Candida* cells must be able to adhere to the intestine. Hyphae have been traditionally shown to have increased adhesion to certain surfaces and mediate biofilm formation that could, in principle, contribute to colonization (Cota and Hoyer, 2015; Lipke, 2018; Verstrepen and Klis, 2006). Most assays in the literature have been performed on abiotic surfaces (such as polystyrene) or simple cellular models that do not mimic the complexity of the gut mucosa. In our *ex vivo* model, we have detected that the μEv93 strain presents a higher adhesion capacity to the mucosa but shows reduced adherence to an abiotic surface, resembling the behavior of CAI4-*WOR1*^{OE} and *hog1*-*WOR1*^{OE} strains (Prieto et al., 2017; Román et al., 2023) and suggesting that adhesins not associated with the filamentous form may be responsible for adhesion to the gut mucosa. As hyphal morphology is a key virulence factor in *C. albicans*, filamentous growth is controlled by a specific humoral antifungal response mediated by sIgAs preferentially directed to this morphology (Doron et al., 2021; Ost et al., 2021) and commensal adaptation should select less pathogenic variants as it has been recently described (Tso et al., 2018). Proteases and phospholipases are well-known virulence factors in *C. albicans* (Schaller et al., 2005) although their potential role as invasins upon gut colonization is still not clear. We observed that micro-evolved strains have lower phospholipase and protease activity; however, this phenomenon may not be due to *WOR1* overexpression as hydrolytic activities are enhanced in a *hog1*-*WOR1*^{OE} (Román et al., 2023). The fact that *FLO8* mutated alleles and an extra copy of *NRG1* which is located in Chr7 are selected variants in micro-evolved strains (this work and Kakade et al., 2023; Tso et al.,

2018) is consistent with the specific genes that these transcriptional factors regulate, which include specific hyphal associated genes, including *SAP4-6* proteinases and *ECE1*, but also hyphal independent SAP genes such as *SAP1* and *SAP3* in the case of *EFG1* or *SAP5* which is repressed by *NRG1* (Ernst, 2000; Felk et al., 2002; Korting et al., 2003; Murad et al., 2001). Low glucose, NAG, and hypoxia are environmental factors present in the gut that can activate the cAMP/PKA pathway. Downstream elements of this pathway, like *Efg1* and *Nrg1*, control the expression of aspartyl proteases such as *Sap7* and *Sap9* or the lipase *Lip4* (Ene et al., 2012).

Microbes entering the gut need to cope with several kinds of environmental stresses, such as oxygen limitation, the presence of bile, osmotic and oxidative stress, and the availability of carbon sources among others. Interestingly, micro-evolved strains did not display improved growth in those conditions *in vitro*, except for bile salts. Micro-evolved strains were also resistant to azoles, a phenotype that fits with the behavior already described for *flo8* mutants (Li et al., 2019). We previously showed that *WOR1* overexpressing cells display an increased susceptibility to bile salts *in vitro*, a feature that has been associated with its reduced colonization levels at early colonization time points and its lower relative proportion in the small intestine but not essential for long-term colonization (Prieto et al., 2017). Micro-evolved strains are markedly resistant to this compound, a phenotype that seems to be independent of *WOR1* but dependent on *FLO8* probably due to the β -mannosylation pattern. This transcription factor activates the expression of *BMT4* and *BMT6* while repressing *BMT2* expression (Polvi et al., 2019), which correlates with the pattern of sensitivity of the corresponding *BMT* mutants. The lack of *Flo8* produces an alteration in mannan exposure at the *C. albicans* surface that is differentially recognized by the α -mannan receptor Dectin-2, involved in immune protection against systemic infection (Lv et al., 2020). It may be tempting to speculate that a hyphal-related *Flo8*-dependent mannosylation pattern would affect the access of bile salts components to the fungal plasma membrane, although *Crz2*, another gene involved in gastrointestinal fitness, also alters resistance to bile and alters cell wall phosphomannan content (Znaidi et al., 2018).

In conclusion, we report here the generation of *C. albicans* strains adapted to the gastrointestinal tract in a commensalism murine model and describe chromosomal reorganizations, some of which perdured in time, that are responsible for this. Our results indicate that inactivation of *Flo8* is a major mechanism of adaptation to the gut of *C. albicans*, although *WOR1* overexpression would also contribute to this phenotype. Both proteins have been related *in vitro* in response to CO_2 via SUMOylation of *Wor1* via *Wos1* in a *Flo8*-dependent manner (Yan et al., 2015) but whether they are both interconnected *in vivo* remains unknown.

All this data let us suggest a tentative model for *C. albicans* colonization where the balance *Wor1*/ *Efg1* may generate *Flo8*^{High} and *Flo8*^{Low} subpopulations with different colonization fitness and *Bmt* expression patterns that confer differential sensitivity to bile salts (Fig. 7).

While our results provide some keys to explain the adaptation of *C. albicans* to the mammalian gastrointestinal tract, it should be kept in mind that microbiome, immune system, and diet profoundly influence the ability of microbes to colonize specific niches and that *C. albicans* is not a natural mice commensal. Validation of these results to humans will surely require alternative and additional experimental approaches.

4. Conclusions

Long-term adaptation of *C. albicans* to the mouse gastrointestinal tract involves permanent and transient chromosomal reorganizations. Loss of function of the *FLO8* gene is partially responsible for increased fitness in the intestine in these strains which show impaired filamentation and resistance to bile salts. An altered β -mannosylation pattern contributes to this bile salt resistance and links gastrointestinal fitness with cell wall architecture.

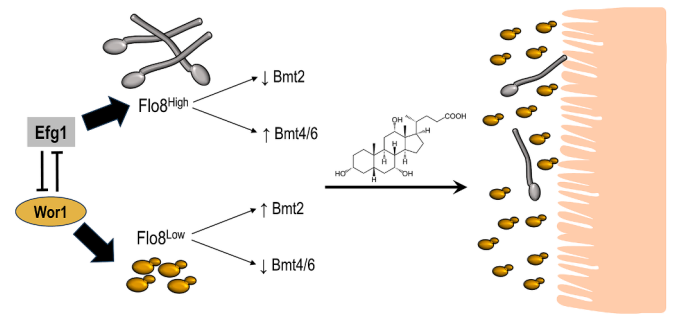


Fig. 7. Model for regulation of gastrointestinal colonization and bile salt sensitivity in *C. albicans*. The transcription factors *Wor1* and *Efg1* repress each other and promote different *C. albicans* phenotypes. The balance of those during colonization would alternate *Flo8*^{High} and *Flo8*^{Low} subpopulations that display different colonization fitness and present alterations in *Bmt* expression conferring them differential bile sensitivity.

5. Material and methods

5.1. Strains and growth conditions

All *C. albicans* strains used in this study are listed in Table 1. Micro-evolved strains were obtained by sequential weekly passages in C57BL/6 mice (see *In vivo* procedures) from the original CAF2-RFP strain. *C. albicans* cells were recovered periodically from stools by plating on YPD media supplemented with chloramphenicol 20 μ g/mL at 37 $^{\circ}$ C. Every 2 months a new set of mice ($n = 2$) were inoculated with colonies from the previous group. The process was repeated for up to 366 days (six groups of mice). Isolated clones were stored in 50 % glycerol at -80 $^{\circ}$ C. For clarity and intuitiveness, we named each clone μ Ev followed by the accumulated number of days that have colonized the mouse gut (μ Ev#). The construction of μ Ev#-*wor1* Δ , *pFLO8* reintegrants, and other control strains are described in the Genetics Procedures section.

Table 1
Candida albicans strains used in this work.

Strain	Genotype	Reference
CA14	<i>ura3::imm434/ura3::imm434 iro1/iro1::imm434</i>	(Fonzi and Irwin, 1993)
CAF2	<i>URA3/ura3::imm434 iro1/iro1::imm434</i>	(Fonzi and Irwin, 1993)
CAF2-RFP	[CAF2] <i>ADH1/adh1::TDH3^{PR}TA TET^{PR}-dTOM2</i>	(Prieto et al., 2014)
CAF2-GFP	[CAF2] <i>ADH1/adh1::TDH3^{PR}TA TET^{PR}-GFP</i>	(Prieto et al., 2014)
<i>flo8</i>	[CA14] <i>flo8/flo8::hisG-URA3-hisG</i>	(Cao et al., 2006)
<i>flo8 eHygB</i>	[<i>flo8</i> Δ / Δ] <i>NEUT5L/neut5L::HygB^R</i>	This work
<i>flo8-pFLO8</i>	[<i>flo8</i> Δ / Δ] <i>NEUT5L/neut5L::FLO8^{PR}-FLO8-HygB^R</i>	This work
BWP17	[CA14] <i>his1::hisG/his1::hisG arg4::hisG/arg4::hisG</i>	(Wilson et al., 1999)
<i>bmt2</i>	[BWP17] <i>bmt2::ARG4/bmt2::HIS1</i>	(Mille et al., 2008)
<i>bmt4</i>	[BWP17] <i>bmt4::ARG4/bmt4::HIS1</i>	(Mille et al., 2008)
<i>bmt6</i>	[BWP17] <i>bmt6Δ::ARG4/bmt6Δ::HIS1</i>	(Mille et al., 2012)
μ Ev93	[CAF2-RFP] *	This work
μ Ev180	[CAF2-RFP] *	This work
μ Ev366	[CAF2-RFP] *	This work
μ Ev93- <i>wor1</i>	[μ Ev93] <i>wor1::SAT1/wor1::SAT1</i>	This work
μ Ev93-pFLO8	[μ Ev93] <i>NEUT5L/neut5L::FLO8^{PR}-FLO8-HygB^R</i>	This work
μ Ev180-pFLO8	[μ Ev180] <i>NEUT5L/neut5L::FLO8^{PR}-FLO8-HygB^R</i>	This work
μ Ev366-pFLO8	[μ Ev366] <i>NEUT5L/neut5L::FLO8^{PR}-FLO8-HygB^R</i>	This work
μ Ev93- <i>wor1</i> -pFLO8	[μ Ev93- <i>wor1</i> Δ / Δ] <i>NEUT5L/neut5L::FLO8^{PR}-FLO8-HygB^R</i>	This work
μ Ev180- <i>wor1</i> -pFLO8	[μ Ev180- <i>wor1</i> Δ / Δ] <i>NEUT5L/neut5L::FLO8^{PR}-FLO8-HygB^R</i>	This work

Cells were routinely grown in liquid YPD medium (2 % glucose, 2 % peptone, 1 % yeast extract) at 37 °C and growth was estimated by O_D₆₀₀ measurements. Microaerophilic or anaerobic atmospheres were achieved in an anaerobic chamber by using commercial systems (GEN-Box Microaer or Anaer, BioMérieux).

To perform the drop tests, 5 µl from suspensions containing approximately 10⁵ stationary cells and from ten-fold serial dilutions were spotted onto solid medium plates (2 % agar). YPD medium was supplemented with phloxine B, hydrogen peroxide, sodium chloride, fluconazole, miconazole, or bile salts (all from Sigma) at the indicated concentrations and incubated for 24 h at 37 °C. Minimal medium (MM) (0.17 % yeast nitrogen base without amino acids, 0.5 % ammonium sulfate) was supplemented with 2 % glycerol, glucose, sodium acetate, sodium citrate, ethanol, or 0.12 % olive oil/0.2 % Tween 80 (Sigma) and incubated for 72 h at 37 °C.

Bile salts sensitivity was also assessed through a CFU viability assay. *C. albicans* cells were incubated for 7 h in YPD broth with or without 0.2 % bile salts. Ten-fold serial dilutions from each culture were spread in YPD-agar plates and incubated at 37 °C for 24 h.

5.2. Genetic procedures

Reintegration of a wild-type *FLO8* version in µEv and *flo8Δ* strains was achieved as follows. *SAT1* selection marker from the pDUP3 plasmid (Gerami-Nejad et al., 2013), digested with *Pme I/Not I*, was replaced by a 2092 bp PCR fragment harboring CaTEF2 promoter-CaHygB-ACT1 terminator from the pLC1031 (Kim et al., 2019) using o-pDUP3-HygB-up and o-pDUP3-HygB-rev primers previously digested with *Pme I/Not I* to generate the pDUP3-HygB plasmid. We amplified a 5363 bp fragment containing a 2296 bp upstream region from the ORF, the *FLO8* ORF and 590 bp of the downstream region from the strain SC5314 by using the primers UP_FLO8XmaI and LO_FLO8NotI. The 5363 bp PCR product was digested with *Xma I/Not I* and accommodated in the pDUP3-HygB previously digested with *Xma I/Not I* generating the pNTHg-*FLO8* plasmid (shortened as pFLO8). Control strains (eHygB) were obtained by integration of pDUP3-HygB. Control (eHygB) and *FLO8* reintegrated strains were obtained by integrating either pNTHg-*FLO8* or pDUP3-HygB digested with *Sfi I* at the *NEUT5L* locus. Transformants were selected on YPD plates supplemented with 400 µg/ml of hygromycin. All *C. albicans* strains were transformed by electroporation using a described procedure (Köhler et al., 1997).

WOR1 deletion in µEv strains was achieved using the Transient CRISPR-Cas9 system that uses separate CaCas9 and sgRNA cassettes as described (Min et al., 2016; Román et al., 2019). The sgRNA expression cassette directed against *WOR1* was constructed by fusing the SNR52 promoter and the sgRNA scaffold in three DNA synthesis steps. In the first step, we amplified SNR52 promoter (PCR1, 1.5 kbp) and sgRNA scaffold and terminator (PCR2, 1 kbp) in two independent PCR from the pV1093 plasmid (Vyas et al., 2015) by using SNR52/F and SNR52/R_WOR1, as primers 1 and 2 for PCR1 and primers SNR52/F_WOR1 and sgRNA/R, as primers 3 and 4 for PCR2. Primers 2 and 3 carry 20 complementary bases of guide sequence that match at position 1346 bp downstream to the starting methionine of *WOR1* ORF. In the second step, primer extension is used to fuse both PCRs. In the third step, we used primers SNR52/N and sgRNA/N to generate the final sgRNA expression cassette. The CaCas9 5.574 kbp cassette was amplified from pV1093 (Vyas et al., 2015) plasmid using primers CaCas9/for and CaCas9/rev. The repair template cassette contains 80-pb arms homologous to sequences upstream and downstream from the *WOR1* coding region and the *SAT1* marker and was amplified using primers WOR1-del_F and WOR1-del_R from pNIM1R-GFP (Prieto et al., 2014) containing the *SAT1* selection marker and 80 bp homologous arms to both sides of *WOR1* ORF. PCR products of CaCas9, sgRNA and *SAT1* repair template cassettes were co-transformed into µEv93 and µEv180 strains and selected on YPD supplemented with 200 µg/ml of nourseothricin. *WOR1* deletion was determined by PCR using genomic DNA and primers

80 bp upstream or downstream to the homologous region Comp_WOR1_F and Comp_WOR1_del_R and a primer complementary to the *SAT1* sequence Comp_SAT1_del_F. Primers are listed in Table 2.

5.3. In vivo procedures

Experiments involving animals were performed in the animal facility at the Medical School of the Universidad Complutense de Madrid following the “Real Decreto 1201/2005, BOE 252” for the Care and Use of Laboratory Animals of the “Ministerio de la Presidencia,” Spain. Animal procedures were approved by the Animal Experimentation Committee of the Universidad Complutense de Madrid and Comunidad de Madrid according to “Artículo 34 del RD 53/2013” (PROEX 226/15 and 320.8/21). The number of animals used was adjusted to a minimum for ethical reasons. All procedures were conducted minimizing mice suffering.

We used the mice commensalism model previously described (Prieto et al., 2014). Briefly, 7–10 weeks-old female mice C57BL/6 (Charles River Laboratories España S.A.U) were pre-treated with an antibiotic combination in the drinking water (2 mg/mL streptomycin, 1 mg/mL bacitracin, and 0.1 mg/mL gentamycin and 0.25 mg/mL fluconazole). Antifungal was removed 24 h before inoculation of a single gavage of 10⁷ *C. albicans* cells in 100 µL of sterile PBS. For competition assays a 1:1 mix from the desired strains was prepared. Fungal levels were quantified by CFU counting from fresh stool samples collected from each mouse every 2–4 days after mechanical homogenization in PBS. Tenfold serial dilutions were plated on SD medium (2 % glucose, 0.5 % (NH₄)₂SO₄, 0.17 % yeast nitrogen base and amino acids, 20 µg/ml chloramphenicol) and incubated for two days.

5.4. Filamentation assays

Filamentation assays in liquid media were performed by inoculation of 1.25 x 10⁶ cells in 2 mL YPD supplemented with 5 % or 100 % FBS (heat-inactivated fetal bovine serum, BioWhittaker). Cells were incubated for 24 h at 37 °C and observed in the microscope. Filamentation on solid media was performed by plating 100 yeast cells onto BSA medium (2 % glucose, 3 % bovine serum albumin, 1.6 % agar, 20 µg/ml chloramphenicol) and after 7 days at 37 °C before scanning.

5.5. Hydrolase activity

To determine phospholipase and protease activity, ~5 × 10⁴ cells from overnight cultures were spread onto MEA (Malt extract agar) 6.5 %; egg-yolk 2 %; NaCl 1–0.5 M; peptone 0.1 %; dextrose 2 %; CaCl₂ 0.055 %, 20 µg/ml chloramphenicol, SEA (Sabouraud chloramphenicol agar) 6.5 %; egg-yolk 2 %; NaCl 1–0.5 M; CaCl₂ 0.0055 %, or BSA (yeast carbon base 1.17 %; YNB 0.01 %; agar 2 %, 20 µg/ml chloramphenicol) agar plates and incubated for 96 h (MEA, SEA) or 120 h (BSA) at 37 °C under normoxia or microaerophilia for 96 h before plates were scanned (Echevarría et al., 2002).

5.6. Adhesion assay

An internal control (CAI4-GFP) was introduced in both biotic and abiotic adhesion assays. Adhesion to large intestine mucosa was assessed as previously described (Prieto et al., 2014). A 1 cm intestinal piece is excised from recently euthanized mice. It was longitudinally opened and washed with PBS before placing it in a 4 mm-diameter methacrylate chamber. A suspension of 2 × 10⁶ of *C. albicans* cells per mL (1:1 mix of the tested strain and the internal control) in RPMI medium is prepared. 10⁵ yeast cells from this suspension were placed in the lumen side and incubated for 150 min at 37 °C. Afterwards, the intestinal tissue is washed with sterile PBS twice to remove non-adhered cells and mechanically disaggregated. Adhesion to polystyrene was performed in 24-well flat bottom plates for cell culture. A suspension of 2 × 10⁴ cells/mL

Table 2
Primers used in this work.

Primer	Sequence (5–3)
o-pDUP3-Hygb-up	ACGTAGATCTGTATAGTGTGCTTGCTGGATATTGC
o-pDUP3-Hygb-rev	AGCTATGGATCATTTTATGATGGAATGAATGGG
UP_FLO8Xmal	CTATCCGGGGCCACATAAGTAGCAACATCAGTG
LO_FLO8NotI	GTTAGCGGGCCAGCCGACGACATGTCATATATGG
SNR52/F	AAGAAAAGAAAAAACCAGGAGTCAA
SNR52/R_WOR1	CCAGTATAATCTGGTTCAATCAATTAATAAATAGTTTACGCAAGTC
SNR52/F_WOR1	AATGAACCGAGTTTACTCTGGTTTTFAGCTAGAAAATAGCAAGTTAAA
sgRNA/R	ACAAATATTTAACTCGGGACCTGG
SNR52/N	GGCGCCGCAAGTGAITAGACT
sgRNA/N	GCAGCTCAGTGAITTAAGAGTAAAGATGG
CaCas9/for	ATCTCAITTAGAATTTGGAACTTTGTGGGTT
CaCas9/rev	TTCCGAGCTCCAAAACCTTCT
WOR1_del_F	ATCTGCTTATATATATTAAGGGGTTGAAAATTTTAAACTGAAAACAACAATTAAGTATAATTCAAATTTAAAGCCGTCAAAACACTAGAGAAATAATAAGAAAAAG
WOR1_del_R	ACACAGACCCACATATATAAGATATACCAATGTAAAAAACAACACTGAATGAGCCCAAAATAATAACAGAAATACACCGGACCCACCTTTGATTGTFAAATAG
Comp_WOR1_F	CCAAITTAAGCCGACAAAAG
Comp_WOR1_del_R	CCCAAAATTTGATTTTTTTTCAGC
Comp_SATI_del_F	CAGGTATAAACTAGACCTCAAAGTCTCG
HWP1-RT-for	TGGTGTATTACTAATCCGG
HWP1-RT-rev	CAATAATAGCAGCAGCGAAG

(1:1 mix of the tested strain and the internal control) in YPD medium is prepared. 10⁴ yeast cells from this suspension were added to each well in YPD medium and incubated for 90 min at 37 °C. After washing 3 times with sterile PBS adhered cells were mechanically detached. In both biotic and abiotic assays, CFU from the adhered fraction was determined on SD plates where strains were differentiated as RFP positive (pink colonies) or negative (white colonies). Adherence is expressed as Adhesion Relative Index (ARI) obtained by dividing the proportion of tested strain in adhered cells by its proportion in the inoculum.

5.7. Genome analysis

Genomic DNA was isolated from stationary phase cells (grown in YPD medium at 37 °C for 18-20 h) using the QIAamp DNA mini kit (Qiagen) according to the provided protocol. The genomes were sequenced at the Biomics platform of Institut Pasteur using the Illumina sequencing technology. Paired-end reads of 150 bp were obtained. Reads have been deposited at the NCBI Sequence Read Archive under BioProject ID PRJNA977487. Analysis of the genome sequencing data used methods detailed elsewhere (Ropars et al., 2018).

5.8. RNA isolation and RT-PCR analysis

Cells grown overnight in YPD at 37 °C were diluted to an O.D.₆₀₀ of 0.1, grown to the exponential phase (O.D.₆₀₀ = 0.8) and collected. RNA was extracted by using nitric acid-treated glass beads in a Fast prep breaker followed by using the RNeasy kit (Qiagen®) according to the manufacturer’s protocol. 1 µg of RNA was used to synthesize cDNA by using the PrimeScript RT kit (Takara). RT-qPCR reactions were prepared using SYBR-Green (PCR Master Mix, Roche). Primers for amplifying *ACT1*, *WOR1*, *ECE1*, and *ALS3* mRNA were already described (Román et al., 2023). Amplification of *HWP1* mRNA was performed with primers in Table 2.

5.9. Statistical analysis

Statistical differences between the two groups were calculated using Student’s two-tailed unpaired t-tests, with alpha = 0.05. Computations assume that samples represent populations with the same scatter (SD). When comparing more than two groups with the control, ordinary one-way ANOVA and Dunnett’s multiple comparisons test were used (alpha = 0.05).

CRediT authorship contribution statement

Susana Hidalgo-Vico: Writing – original draft, Methodology, Investigation, Formal analysis, Conceptualization. **Daniel Prieto:** Writing – review & editing, Writing – original draft, Visualization, Methodology, Investigation, Formal analysis, Conceptualization. **Rebeca Alonso-Monge:** Writing – review & editing, Supervision, Project administration, Funding acquisition, Conceptualization. **Elvira Román:** Writing – review & editing, Supervision, Formal analysis, Conceptualization. **Corinne Maufrais:** Writing – original draft, Methodology, Investigation, Formal analysis. **Christophe d’Enfert:** Writing – review & editing, Writing – original draft, Supervision, Project administration, Funding acquisition, Conceptualization. **Jesús Pla:** Writing – review & editing, Writing – original draft, Supervision, Project administration, Funding acquisition, Formal analysis, Conceptualization.

Funding

This work was supported in the laboratory of JP by Ministerio de Ciencia e Innovación [grant number PID2021-122648NB-I00]; and Comunidad de Madrid [grant number PR38/21-32] and in the laboratory of CdE by the Agence Nationale de Recherche [ANR-10-LABX-62-IBEID]. We are grateful to S. Azebi for genome sequencing (Biomics

Platform, C2RT, Institut Pasteur, Paris, France) supported by France Génomique [ANR-10-INBS-09-09] and IBISA.

Declaration of competing interest

The authors declare that they have no known competing financial interests or personal relationships that could have appeared to influence the work reported in this paper.

Acknowledgements

We would like to thank Grace Parry for language proofreading.

Appendix A. Supplementary data

Supplementary data to this article can be found online at <https://doi.org/10.1016/j.fgb.2024.103939>.

References

- Alonso-Monge, R., et al., 2021a. *Candida albicans* colonization of the gastrointestinal tract: a double-edged sword. *PLoS Pathog.* 17, e1009710.
- Alonso-Monge, R., et al., 2021b. Identification of Clinical Isolates of *Candida albicans* with Increased Fitness in Colonization of the Murine Gut. *J. Fungi* 7, 695.
- Bendel, C.M., et al., 2002. Cecal colonization and systemic spread of *Candida albicans* in mice treated with antibiotics and dexamethasone. *Pediatr. Res.* 51, 290–295.
- Bouchonville, K., et al., 2009. Aneuploid chromosomes are highly unstable during DNA transformation of *Candida albicans*. *Eukaryot Cell.* 8, 1554–1566.
- Cao, F., et al., 2006. The Flo8 transcription factor is essential for hyphal development and virulence in *Candida albicans*. *Mol. Biol. Cell* 17, 295–307.
- Cota, E., Hoyer, L.L., 2015. The *Candida albicans* agglutinin-like sequence family of adhesins: functional insights gained from structural analysis. *Future Microbiol.* 10, 1635.
- Courjol, F., et al., 2015. Beta-1,2-mannosyltransferases 1 and 3 participate in yeast and hyphae O- and N-linked mannosylation and alter *Candida albicans* fitness during infection. *Open Forum. Infect Dis.* 2, ofv116.
- de Groot, P.W., et al., 2013. Adhesins in human fungal pathogens: glue with plenty of stick. *Eukaryot. Cell* 12, 470–481.
- Domagk, D., et al., 2001. Common bile duct obstruction due to candidiasis. *Scand. J. Gastroenterol.* 36, 444–446.
- Doron, I., et al., 2021. Mycobiota-induced IgA antibodies regulate fungal commensalism in the gut and are dysregulated in Crohn's disease. *Nat. Microbiol.* 6, 1493–1504.
- Du, H., et al., 2012. The transcription factor Flo8 mediates CO₂ sensing in the human fungal pathogen *Candida albicans*. *Mol. Biol. Cell.* 23, 2692–2701.
- Echevarría, A., et al., 2002. Estudio comparativo de dos medios de cultivo para la detección de la actividad fosfolipasa en cepas de *Candida albicans* y *Cryptococcus neoformans*. *Rev. Iberoam. Microb.* 19, 95–98.
- Eckstein, M.T., et al., 2020. Gut bacteria shape intestinal microhabitats occupied by the fungus *Candida albicans*. *Curr. Biol.*
- Ene, I.V., et al., 2012. Carbon source-induced reprogramming of the cell wall proteome and secretome modulates the adherence and drug resistance of the fungal pathogen *Candida albicans*. *Proteomics* 12, 3164–3179.
- Ene, I.V., et al., 2018. Global analysis of mutations driving microevolution of a heterozygous diploid fungal pathogen. *Proc. Natl. Acad. Sci. U.S.A.* 115, E8688–E8697.
- Ernst, J.F., 2000. Transcription factors in *Candida albicans* - environmental control of morphogenesis. *Microbiology (Reading)* 146 (Pt 8), 1763–1774.
- Felk, A., et al., 2002. *Candida albicans* hyphal formation and the expression of the Efg1-regulated proteinases Sap4 to Sap6 are required for the invasion of parenchymal organs. *Infect Immun.* 70, 3689–3700.
- Forche, A., et al., 2009. Evolution in *Candida albicans* populations during a single passage through a mouse host. *Genetics* 182, 799–811.
- Forche, A., et al., 2018. Rapid phenotypic and genotypic diversification after exposure to the oral host niche in *Candida albicans*. *Genetics* 209, 725–741.
- Forche, A., et al., 2019. Selection of *Candida albicans* trisomy during oropharyngeal infection results in a commensal-like phenotype. *PLoS Genet.* 15, e1008137.
- Fox, E.P., et al., 2015. An expanded regulatory network temporally controls *Candida albicans* biofilm formation. *Mol. Microbiol.* 96, 1226–1239.
- Gerami-Nejad, M., et al., 2013. Shuttle vectors for facile gap repair cloning and integration into a neutral locus in *Candida albicans*. *Microbiology* 159, 565–579.
- Guinan, J., et al., 2018. Secondary bile acids inhibit *Candida albicans* growth and morphogenesis. *Pathog. Dis.* 76.
- Hidalgo-Vico, S., et al., 2022. Overexpression of the white opaque switching master regulator *wor1* alters lipid metabolism and mitochondrial function in *Candida albicans*. *J. Fungi (Basel)* 8.
- Hoyer, L.L., Cota, E., 2016. *Candida albicans* agglutinin-like sequence (Als) family vignettes: a review of als protein structure and function. *Front. Microbiol.* 7, 280.
- Hsieh, S.H., et al., 2017. Encapsulation of antifungals in micelles protects *Candida albicans* during gall-bladder infection. *Front. Microbiol.* 8, 117.
- Huang, G., et al., 2006. Bistable expression of *WOR1*, a master regulator of white-opaque switching in *Candida albicans*. *Proc. Natl. Acad. Sci. U.S.A.* 103, 12813–12818.
- Kakade, P., et al., 2023. Aneuploidy and gene dosage regulate filamentation and host colonization by *Candida albicans*. *Proc. Natl. Acad. Sci. U.S.A.* 120, e2218163120.
- Kim, S.H., et al., 2019. Genetic analysis of *Candida auris* implicates Hsp90 in morphogenesis and azole tolerance and Cdr1 in azole resistance. *MBio* 10.
- Koh, A.Y., 2013. Murine models of *Candida* gastrointestinal colonization and dissemination. *Eukaryot. Cell* 12, 1416–1422.
- Köhler, G.A., et al., 1997. Overexpression of a cloned IMP dehydrogenase gene of *Candida albicans* confers resistance to the specific inhibitor mycophenolic acid. *J. Bacteriol.* 179, 2331–2338.
- Korting, H.C., et al., 2003. Reduced expression of the hyphal-independent *Candida albicans* proteinase genes *SAP1* and *SAP3* in the *efg1* mutant is associated with attenuated virulence during infection of oral epithelium. *J. Med. Microbiol.* 52, 623–632.
- Leonardi, I., et al., 2018. CX3CR1(+) mononuclear phagocytes control immunity to intestinal fungi. *Science* 359, 232–236.
- Li, W.J., et al., 2019. *FLO8* deletion leads to azole resistance by upregulating *CDR1* and *CDR2* in *Candida albicans*. *Res. Microbiol.* 170, 272–279.
- Liang, S.H., et al., 2019. Hemizyosity enables a mutational transition governing fungal virulence and commensalism. *Cell Host Microbe.* 25 (418–431), e6.
- Lipke, P.N., 2018. What we do not know about fungal cell adhesion molecules. *J. Fungi (Basel)* 4.
- Liu, J.Y., et al., 2015. Mutations in the Flo8 transcription factor contribute to virulence and phenotypic traits in *Candida albicans* strains. *Microbiol. Res.* 178, 1–8.
- Lv, Q.Z., et al., 2020. Priming with *FLO8*-deficient *Candida albicans* induces Th1-biased protective immunity against lethal polymicrobial sepsis. *Cell Mol. Immunol.*
- Marco, F., et al., 1999. Elucidating the origins of nosocomial infections with *Candida albicans* by DNA fingerprinting with the complex probe Ca3. *J. Clin. Microbiol.* 37, 2817–2828.
- Min, K., et al., 2016. *Candida albicans* gene deletion with a transient CRISPR-Cas9 system. *mSphere* 1.
- Miranda, L.N., et al., 2009. *Candida* colonisation as a source for candidaemia. *J. Hosp. Infect.* 72, 9–16.
- Murad, A.M., et al., 2001. NRG1 represses yeast-hypha morphogenesis and hypha-specific gene expression in *Candida albicans*. *EMBO J.* 20, 4742–4752.
- Neville, B.A., et al., 2015. *Candida albicans* commensalism in the gastrointestinal tract. *FEMS Yeast Res.* 15.
- Noble, S.M., 2013. *Candida albicans* specializations for iron homeostasis: from commensalism to virulence. *Curr. Opin. Microbiol.* 16, 708–715.
- Ost, K.S., et al., 2021. Adaptive immunity induces mutualism between commensal eukaryotes. *Nature*.
- Pande, K., et al., 2013. Passage through the mammalian gut triggers a phenotypic switch that promotes *Candida albicans* commensalism. *Nat. Genet.* 45, 1088–1091.
- Perez, J.C., et al., 2013. *Candida albicans* commensalism and pathogenicity are intertwined traits directed by a tightly knit transcriptional regulatory circuit. *PLoS Biol.* 11, e1001510.
- Pierce, J.V., et al., 2013. Normal adaptation of *Candida albicans* to the murine gastrointestinal tract requires Efg1p-dependent regulation of metabolic and host defense genes. *Eukaryot. Cell* 12, 37–49.
- Pierce, J.V., Kumamoto, C.A., 2012. Variation in *Candida albicans* *EFG1* expression enables host-dependent changes in colonizing fungal populations. *MBio* 3, e00117–e00212.
- Polvi, E.J., et al., 2019. Functional divergence of a global regulatory complex governing fungal filamentation. *PLoS Genet.* 15, e1007901.
- Poullain, D., Jouault, T., 2004. *Candida albicans* cell wall glycans, host receptors and responses: elements for a decisive crosstalk. *Curr. Opin. Microbiol.* 7, 342–349.
- Prieto, D., et al., 2014. The HOG pathway is critical for the colonization of the mouse gastrointestinal tract by *Candida albicans*. *PLoS One* 9, e87128.
- Prieto, D., et al., 2016. Adaptation of *Candida albicans* to commensalism in the gut. *Future Microbiol.* 11, 567–583.
- Prieto, D., et al., 2017. Overexpression of the transcriptional regulator *WOR1* increases susceptibility to bile salts and adhesion to the mouse gut mucosa in *Candida albicans*. *Front. Cell. Infect. Microbiol.* 7, 389.
- Prieto, D., Pla, J., 2022. Comparative analysis of the fitness of *Candida albicans* strains during colonization of the mice gastrointestinal tract. *Methods Mol. Biol.* 2542, 233–244.
- Ramírez-Zavala, B., et al., 2017. The Snf1-activating kinase Sak1 is a key regulator of metabolic adaptation and in vivo fitness of *Candida albicans*. *Mole. Microbiol. n/a/n/a*.
- Román, E., et al., 2018. *TUP1*-mediated filamentation in *Candida albicans* leads to inability to colonize the mouse gut. *Future Microbiol.* 13, 857–867.
- Román, E., et al., 2019. Implementation of a CRISPR-based system for gene regulation in *Candida albicans*. *mSphere* 4.
- Román, E., et al., 2023. The defective gut colonization of *Candida albicans* *hog1* MAPK mutants is restored by overexpressing the transcriptional regulator of the white opaque transition *WOR1*. *Virulence* 14, 2174294.
- Ropars, J., et al., 2018. Gene flow contributes to diversification of the major fungal pathogen *Candida albicans*. *Nat. Commun.* 9, 2253.
- Schaller, M., et al., 2005. Hydrolytic enzymes as virulence factors of *Candida albicans*. *Mycoses* 48, 365–377.
- Selmecki, A., et al., 2006. Aneuploidy and isochromosome formation in drug-resistant *Candida albicans*. *Science* 313, 367–370.
- Selmecki, A.M., et al., 2009. Acquisition of aneuploidy provides increased fitness during the evolution of antifungal drug resistance. *PLoS Genet.* 5.

- Soll, D.R., 2014. The role of phenotypic switching in the basic biology and pathogenesis of *Candida albicans*. *J. Oral. Microbiol.* 6.
- Sonneborn, A., et al., 1999. Control of white-opaque phenotypic switching in *Candida albicans* by the Efg1p morphogenetic regulator. *Infect. Immun.* 67, 4655–4660.
- Srikantha, T., et al., 2006. *TOS9* regulates white-opaque switching in *Candida albicans*. *Eukaryot. Cell* 5, 1674–1687.
- Stoldt, V.R., et al., 1997. Efg1p, an essential regulator of morphogenesis of the human pathogen *Candida albicans*, is a member of a conserved class of bHLH proteins regulating morphogenetic processes in fungi. *EMBO J.* 16, 1982–1991.
- Sun, L.L., et al., 2023. Aneuploidy mediates rapid adaptation to a subinhibitory amount of fluconazole in *Candida albicans*. *Microbiol Spectr.* 11, e0301622.
- Tso, G.H.W., et al., 2018. Experimental evolution of a fungal pathogen into a gut symbiont. *Science* 362, 589–595.
- Vautier, S., et al., 2015. *Candida albicans* colonization and dissemination from the murine gastrointestinal tract: the influence of morphology and Th17 immunity. *Cell. Microbiol.* 17, 445–450.
- Verstrepen, K.J., Klis, F.M., 2006. Flocculation, adhesion and biofilm formation in yeasts. *Mol. Microbiol.* 60, 5–15.
- Vyas, V.K., et al., 2015. A *Candida albicans* CRISPR system permits genetic engineering of essential genes and gene families. *Sci. Adv.* 1, e1500248.
- Witchley, J.N., et al., 2019. *Candida albicans* morphogenesis programs control the balance between gut commensalism and invasive infection. *Cell Host Microbe.* 25 (432–443), e6.
- Yan, M., et al., 2015. SUMOylation of Wor1 by a novel SUMO E3 ligase controls cell fate in *Candida albicans*. *Mol. Microbiol.* 98, 69–89.
- Zhai, B., et al., 2020. High-resolution mycobiota analysis reveals dynamic intestinal translocation preceding invasive candidiasis. *Nat Med.* 26, 59–64.
- Znaidi, S., et al., 2018. Systematic gene overexpression in *Candida albicans* identifies a regulator of early adaptation to the mammalian gut. *Cell Microbiol.*
- Zordan, R.E., et al., 2006. Epigenetic properties of white-opaque switching in *Candida albicans* are based on a self-sustaining transcriptional feedback loop. *Proc. Natl. Acad. Sci. U. S. A.* 103, 12807–12812.